Received: 8 October 2020 | Revised: 5 November 2020

DOI: 10.1111/mmi.14641

RESEARCH ARTICLE

WILEY

The soluble cytoplasmic N-terminal domain of the FocA channel gates bidirectional formate translocation

Michelle Kammel | Doreen Hunger | Robert Gary Sawers

Institute of Microbiology, Martin-Luther University Halle-Wittenberg, Halle (Saale), Germany

Correspondence
R. Gary Sawers, Institute of Microbiology, Martin-Luther University Halle-Wittenberg, Kurt-Mothes-Str. 3, 06120 Halle (Saale) Germany.
Email: gary.sawers@mikrobiologie.uni-halle.de

Present address
Doreen Hunger, IDT Biologika, Dessau-Roßlau, Germany

Funding information
Deutsche Forschungsgemeinschaft, Grant/Award Number: GRK1026

Abstract

FocA belongs to the pentameric FNT (formate-nitrite transporter) superfamily of anion channels, translocating formate bidirectionally across the cytoplasmic membrane of *Escherichia coli* and other microorganisms. While the membrane-integral core of FocA shares considerable amino acid sequence conservation with other FNT family members, the soluble cytoplasmic N-terminal domain does not. To analyze the potential biochemical function of FocA's N-terminal domain in vivo, we constructed truncation derivatives and amino acid-exchange variants, and determined their ability to translocate formate across the membrane of *E. coli* cells by monitoring intracellular formate levels using a formate-sensitive reporter system. Analysis of strains synthesizing these FocA variants provided insights into formate efflux. Strains lacking the ability to generate formate intracellularly allowed us to determine whether these variants could import formate or its toxic chemical analog hypophosphite. Our findings reveal that the N-terminal domain of FocA is crucial for bidirectional FocA-dependent permeation of formate across the membrane. Moreover, we show that an amino acid sequence motif and secondary structural features of the flexible N-terminal domain are important for formate translocation, and efflux/influx is influenced by pyruvate formate-lyase. The soluble N-terminal domain is, therefore, essential for bidirectional formate translocation by FocA, suggesting a "gate-keeper" function controlling anion accessibility.

KEYWORDS
anion gating, FNT channel, formate permeation, hypophosphite-sensitivity, N-terminal domain

1 | INTRODUCTION

FNT (formate-nitrite transporter) channels represent a family of evolutionarily ancient membrane proteins that selectively permeate monovalent anions such as formate, nitrite, lactate, or hydrosulfide across cytoplasmic membranes (Lü et al., 2013; Waight et al., 2013). Phylogenomic analyses (Mukherjee et al., 2017; Saier et al., 1999) have shown that FNT channels are widespread in Bacteria, Euryarchaeota, and in certain fungi, yeasts, and protists, including *Plasmodium* and *Toxoplasma* species. They are not present in higher Eukarya and they thus represent potentially important drug targets in pathogens (Golldack et al., 2017; Hapuarachchi et al., 2017). The first FNT to be identified and characterized as an anion channel was FocA of *Escherichia coli*, which bidirectionally translocates formate (Suppmann & Sawers, 1994). Significant advances were made in

our understanding of these proteins around 10 years ago when detailed structural analyses of several FNT channels revealed that all have in common a homopentameric organization, with an overall fold that is structurally similar to aqua- and glyceroporins (Czyzewski & Wang, 2012; Lü et al., 2011, 2012b; Waight et al., 2010; Wang et al., 2009). Each monomer comprises 6 transmembrane helices (TM), two of which, helices 2 and 5, are broken centrally and fold to form a pore through the monomer. This substrate pore (Waight et al., 2010, 2013; Wang et al., 2009), which has an "hourglass" shape, includes a narrow passage bounded by hydrophobic cytoplasmic and periplasmic constriction sites, which are suggested to act as anion-selectivity filters (Lü et al., 2013; Waight et al., 2013). Molecular dynamic simulations (Atkovska & Hub, 2017; Lv et al., 2013), as well as structural analyses indicate that this pore does not allow passage of water and it is too hydrophobic to allow permeation of an anion, implying that undissociated formic acid is translocated through FocA. Access to the formate-selectivity filters is via funnel-like vestibules on the cytoplasmic and periplasmic sides of the membrane and a portion of the broken TM2 forms an Ω-loop that is inserted within the cytoplasmic funnel forming a "plug"-like structure restricting access to the narrow pore (Waight et al., 2013). The tip of the Ω-loop includes a highly conserved threonyl residue that forms a hydrogen-bond with a conserved histidinyl residue, which closes the narrow hydrophobic pore. Together, the Ω-loop and the histidinyl residue have been proposed to "gate" access of the anion to the pore. How this gate is opened and closed, however, is still unresolved, but it has been suggested (Waight et al., 2013) that protonation of the central histidinyl residue would release the hydrogen-bonded Thr and cause movement of the Ω-loop out of the cytoplasmic vestibule and some structures of FocA support this model (Lü et al., 2011). This model would also be in accord with the pH-sensitivity of FocA, whereby at pH above 6.5 formate is translocated out of the cytoplasm and at a pH below 6.5, formate is imported into the cell (Lü et al., 2011; Suppmann & Sawers, 1994; Wang et al., 2009). The problem with this model is that, unlike FocA, the NirC (nitrite reduction protein C) and HSC (hydrosulfide ion channel) membrane channels show no evidence of pH-sensitive anion translocation, yet, they also possess the conserved His and Thr residues (Czyzewski & Wang, 2012; Lü et al., 2012b). This suggests that FNT channels might have a second gating mechanism to move the Ω-loop out of the cytoplasmic vestibule.

While the six membrane-integral TMs of each FNT monomer exhibit an overall conservation at the primary through quaternary structural levels (Hunger et al., 2017; Lü et al., 2013; Waight et al., 2013), the soluble N-terminal domain of these proteins exhibits only very limited similarity between different family members, both in terms of length and amino acid sequence (Figure 1a). For example, the N-terminal domain of FocA from *E. coli* is around 31 amino acid residues in length, while the same domain of NirC from *E. coli* and that of HSC from *Clostridioides difficile* are only 23–24 residues in length; and some of these N-terminal domains are even shorter (Mukherjee et al., 2017). A common general feature of these soluble N-terminal domains, however, is that they include short α-helices, which in the case of NirC and HSC are found to lie parallel to the membrane (Czyzewski & Wang, 2012; Lü et al., 2012), forming a rigid structure near the entrance to the cytoplasmic vestibule of the pore. Because the N-terminal domain of these proteins can contact TM2b, and thus, influence the position within the vestibule of the Ω-loop, it has been suggested (Czyzewski & Wang, 2012; Waight et al., 2013; Figure 1b) that the N-terminal domain might modulate formate accessibility to the pore. Indeed, the initial structure of FocA from *E. coli* was obtained with a protein lacking the first 21 amino acid residues of the N-terminal domain and all five pores in this structure were in the closed conformation (Wang et al., 2009). Together, these structural analyses suggest one of two functions for the N-terminal domain; either it acts as an anchor to stabilize the core of the protein in the membrane, or it functions as an interaction platform for a cytoplasmic protein(s) that might control opening and closing of the pore. We have previously shown using combined in vitro chemical cross-linking and high-resolution mass spectrometry that the cytoplasmic enzyme pyruvate formate-lyase (PflB) of *E. coli* interacts specifically with FocA, with the majority of cross-links occurring at the N-terminal domain (Doberenz et al., 2014). Moreover, PflB, which exists in conformationally different active and inactive forms (Knappe & Sawers, 1990; Peng et al., 2010), generates the substrate for FocA; the *focA* and *pflB* genes are also adjacent and co-expressed on the *E. coli* chromosome (Sawers & Böck, 1989). Notably, the genes encoding several other FNTs, such as NirC, FdhC (formate dehydrogenase channel C), and HSC, are located adjacent, or in proximity, to genes encoding the enzymes that generate their respective anion substrates (Czyzewski & Wang, 2012; Peakman et al., 1990; White & Ferry, 1992). This might suggest that perhaps an interaction between the FNT channel and an enzyme that generates its cognate substrate could also be considered for other systems. Nevertheless, in vivo data in support of such an hypothesis are currently only circumstantial.

Studying FNT channel function in vivo is inherently difficult due to the biochemistry of these proteins and the lack of a suitable assay system to monitor accurately and quantitatively monovalent anion permeation in whole cells. Nevertheless, some progress has been made by studying FocA in its homologous host (Beyer et al., 2013; Hunger et al., 2014, 2017; Suppmann & Sawers, 1994) and FocA and other FNTs in heterologous systems such as yeast (Erler et al., 2018; Wiechert & Beitz, 2017), which do not have FNT channels. In vitro studies using electrophysiology of isolated FNT channels (Lü et al., 2011, 2012b) have revealed that the proteins show poly-specificity with regard to anion permeation, leading to the suggestion that enterobacterial FocA translocates the anionic products of mixed-acid fermentation out of the cell (Lü et al., 2012a). This contradicts physiological studies for FocA in *E. coli*, however, which indicate that FocA is specific for the bidirectional permeation of formate (Beyer et al., 2013; Hunger et al., 2014, 2017; Suppmann & Sawers, 1994). Hence, both in vitro and heterologous expression studies might be potentially limited by the inherent absence of the natural physiological and biochemical environment in which these proteins function. In this study, we present evidence that the N-terminal domain of FocA from *E. coli* is essential for bidirectional permeation of formate, and indeed for uptake of the toxic formate analog hypophosphite. Together, our data suggest different mechanisms for formate efflux and influx and that the N-terminal domain, along with PflB, might have a role in gating formate access. Data obtained using N-terminally truncated derivatives are also consistent with a role of the N-terminal domain in stabilizing FocA in the membrane. To our knowledge, this

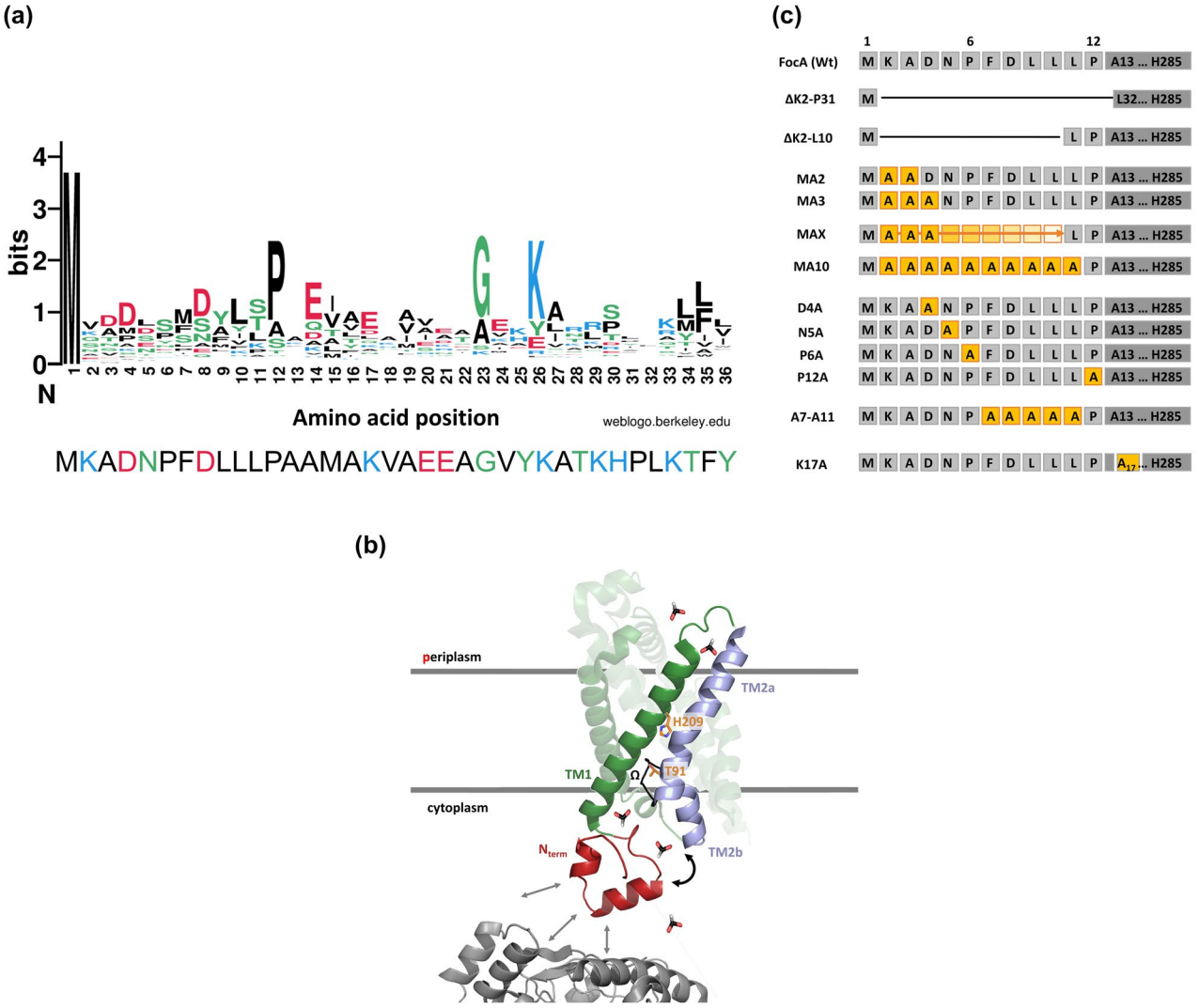

FIGURE 1 Amino acid residues of the N-terminal domain of FocA. (a) Conservation plot comparing the first 36 N-terminal amino acid residues from 258 FNT channels using the WebLogo 3 stacking algorithm (Crooks et al., 2004). Amino acids displayed in black possess an unpolar side chain (A, F, I, L, M, V, W) and polar side chains are indicated in green (G, S, T, N, Q, Y). Acidic amino acids are shown in red (D, E) and alkaline residues in blue (H, K, R). The plot is with reference to the amino acid sequence of the N-terminal region of native FocA from *E. coli*, the sequence of which is presented below the plot. (b) Schematic representation of a single FocA monomer in the membrane (green and blue, pdb 3KCU, amino acids 29–285) illustrating how the N-terminal domain (red, de novo modeled by PEP-FOLD 3.5, amino acids 1–28) might control the conformational change of the Ω-loop (black) through contacting the transmembrane helix TM2b (light blue). Permeation of formate ions across the cytoplasmic membrane is shown schematically. Residues essential for the translocation mechanism, His209 and Thr91, are highlighted in orange. Interaction of FocA´s N-terminal domain with PflB (gray, pdb 1H18) is shown at the bottom left. (c) Scheme depicting representative examples of amino acid exchanges/deletions introduced into the N-terminal domain of FocA variants and their corresponding nomenclature. The X and the horizontal arrow (row labeled MAX) indicate successive exchanges MA4 through MA9

study presents the first in vivo data suggesting that a soluble N-terminal domain of an anion channel is involved in mediating anion permeation.

2 | RESULTS

2.1 | N-terminally truncated FocA variants are impaired in formate efflux

In order to examine the functional significance of the soluble, cytoplasmically oriented, N-terminal domain of FocA on formate translocation, we made use of a single-copy *fdhF*$_p$::*lacZ* reporter, which responds to changes in the intracellular formate concentration (Beyer et al., 2013; Hunger et al., 2014). The wild-type strain DH4100 grown anaerobically in M9-glucose medium produced formate from pyruvate and had a β-galactosidase enzyme activity of ~580 Miller units (Figure 2a). Under the same growth conditions, strain DH201 (Δ*pflB*), which lacks the enzyme pyruvate formate-lyase (PflB), has a β-galactosidase enzyme activity of less than 10 units. Strain DH701 (*focA*) cannot synthesize the formate channel FocA, and thus, accumulates formate intracellularly when compared with wild type, resulting in an increased β-galactosidase enzyme activity of ~700 Miller units

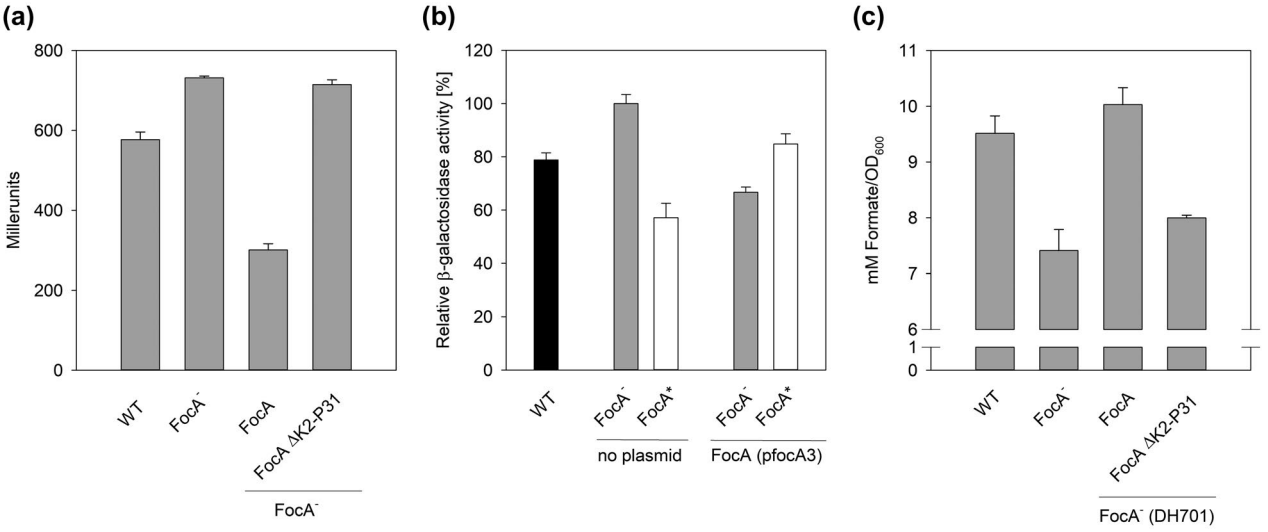

FIGURE 2 The soluble N-terminal domain of FocA is essential for formate efflux. β-galactosidase enzyme activities are shown after anaerobic growth in glucose-minimal medium (see Experimental procedures). (a) The *focA* mutant DH701 (FocA$^-$) transformed with a plasmid carrying a *focA* gene encoding either C-terminally strep-tagged native FocA (pfocA3) or a variant lacking amino acid residues 2 through 31 (FocAΔK2-P31) was analyzed. WT = DH4100. (b) The indicated strains were analyzed either without or after transformation with plasmid pfocA3, encoding strep-tagged native FocA. WT, DH4100 (black histogram); FocA$^-$, DH701 (*focA*) (gray histogram); FocA*, DH702 (FocA overproduced; white histogram) were measured without a plasmid, or after transformation with pfocA3. About 100% β-galactosidase enzyme activity was determined for strain DH701 to be 620 ± 21 Miller units. (c) The concentration of formate in the culture medium after anaerobic growth in glucose-minimal medium was determined by HPLC analysis (see Experimental procedures) for the indicated strains. WT, DH4100; FocA$^-$, DH701 (*focA*); FocA$^-$/FocA, DH701/pfocA3; FocA$^-$/FocAΔK2P31, DH701/pfocAΔK2P31. All experiments were performed with minimally three biological replicates, each assay performed in triplicate

relative to the wild-type strain DH4100 (Figure 2a). Synthesis of the native FocA protein with a *C*-terminal strep-tag, encoded on plasmid pfocA3 (Table S2), in strain DH701 lowered intracellular formate levels compared to the FocA-free strain, which is reflected in an approximate 2.5-fold reduction in β-galactosidase enzyme activity after anaerobic fermentative growth (Figure 2a). Increasing the abundance of FocA 10- to 20-fold by converting the GUG translation initiation codon of single-copy *focA* to the more efficient AUG (Suppmann & Sawers, 1994; see also Figure 2b) in strain DH702 does not significantly impact the formate export kinetics (Suppmann & Sawers, 1994) or the formate-dependent β-galactosidase enzyme activity (Figure 2b); introduction of pfocA3 carrying the *focA* gene encoding C-terminally strep-tagged FocA into DH702 caused only an approximate 20% increase in *fdhF*$_p$::*lacZ* expression. This result indicates that the amount of FocA in the anaerobic cell does not limit formate translocation, but at the same time indicates that increasing the abundance of the protein does not significantly affect formate efflux (Beyer et al., 2013; Suppmann & Sawers, 1994). This is consistent with the protein having a channel function, and validates the use of plasmid-borne *focA* expression to examine the effects of amino acid exchanges on translocation activity in vivo. Moreover, the presence of these plasmids in DH701 had no impact on the levels of PflB, the enzyme that synthesizes formate during anaerobic growth (Figure S1).

In an initial experiment to analyze whether the soluble, cytoplasmic domain of FocA is important for FocA function, a plasmid carrying a modified *focA* gene encoding FocA variant (FocAΔK2-P31) that lacked the complete N-terminal domain (removal of amino acid residues K2-P31; Figure 1c) was constructed. Introduction of pfocAΔK2-P31, whose modified *focA* gene encodes FocAΔK2-P31, into strain DH701 (*focA*) failed to result in a significant reduction in β-galactosidase enzyme activity compared to the enzyme activity measured in DH701, and by extension intracellular formate levels, to the levels observed when plasmid-encoded native FocA was introduced into the strain (Figure 2a). This suggests that this truncated FocA variant is impaired in formate efflux.

To examine whether removal of the N-terminal domain indeed affected formate efflux by FocA, we determined the formate concentration in the medium after fermentative growth to the late exponential phase (OD_{600} = 0.8) (Figure 2c). The results show that strain DH701 (*focA*) exported approximately 20%–25% less formate compared with the wild-type strain DH4100 and DH701 transformed with pfocA3. Introduction of plasmid pfocAΔK2-P31 into DH701 revealed formate levels in the growth medium were in a range similar to those of the *focA* mutant, supporting the notion that formate export is impaired in a FocA variant lacking the N-terminus. Note that there is minimally one further, as yet unidentified, system present in *E. coli* that can translocate formate (Suppmann & Sawers, 1994). NirC can be ruled out as the unidentified formate channel/transporter because a *focA-nirC* double-null mutant retains the formate-translocating capability of a *focA* mutant (Beyer et al., 2013; Suppmann, 1993). Together, these results reveal an inverse relationship between intracellular β-galactosidase activities and extracellular formate concentration, and are consistent with the N-terminally truncated FocA derivative being impaired in formate efflux.

2.2 | N-terminal truncation variants are synthesized but are less stable than native FocA

To analyze whether the truncated FocAΔK2-P31 variant formed membrane-integral homopentamers, which is characteristic for the wild-type FocA protein (Falke et al., 2010; Hunger et al., 2017), a C-terminally strep-tagged variant of FocAΔK2-P31 was purified (see Experimental procedures) and electrophoretically separated in SDS- and BN- (blue-native) PAGE (Figure 3a,b). SDS-PAGE revealed that native, strep-tagged FocA migrated with a molecular mass of approximately 23 kDa, despite the deduced molecular mass of the protein being 32.2 kDa with the strep-tag, as has been previously reported (Falke et al., 2010), while the N-terminally truncated FocAΔK2-P31 variant migrated slightly faster (Figure 3a), consistent with the reduction in the length of FocA by 30 amino acid residues (deduced mass of monomer = 29.01 kDa with a tag). Importantly, both proteins migrated in BN-PAGE as pentamers, albeit FocAΔK2-P31 (deduced mass of strep-tagged pentamer = 145.1 kDa) migrated slightly faster than the native, recombinant protein (deduced mass of strep-tagged pentamer = 161 kDa) (Figure 3b). A further N-terminally truncated derivative of FocA, FocAΔK2-L10, was constructed (Figure 1c) and a strep-tagged variant of this protein was also purified and analyzed by BN-PAGE (Figure 3b). The protein migrated like FocAΔK2-P31 as a homopentamer. When a plasmid encoding FocAΔK2-L10 (Figure 1c) was introduced into DH701 β-galactosidase activity was recorded as 648 Miller units, indicating that it was also impaired in formate efflux.

While approximately 0.6 mg of native strep-tagged FocA was isolated per L of culture, in comparison, only 0.2 mg/L of FocAΔK2-P31 and 0.1 mg/L of FocAΔK2-L10 was isolated, suggesting that the truncated variants are less stable, or less efficiently inserted into the membrane, than the full-length protein. In order to test this, membrane fractions isolated from strains DH4100 (wild type), DH701/pfocA3, and DH701/pfocAΔK2-P31 were separated by SDS-PAGE and treated with anti-FocA antibodies in a western blot (Figure S2a). The blot revealed that FocA encoded by the recombinant *focA* gene on pfocA3 migrated with a mass of approximately 24 kDa in the Tris-tricine gel system. The level of wild type, chromosomally encoded FocA in DH4100 was significantly lower and migrated slightly faster than the strep-tagged recombinant protein, which has also been reported previously (Falke et al., 2010; Hunger et al., 2017). In contrast, the truncated variant FocAΔK2-P31 could not be detected after growth in glucose-minimal medium. Note that the weak band observed in an extract from DH701 (*focA*), and which migrated slightly above FocA in the Tris-tricine gel system (Figure S2a), is a cross-reacting polypeptide of unknown origin that occasionally obscures the migration position of FocA (Falke et al., 2010). In standard SDS-PAGE analysis, this cross-reacting species migrates slightly faster than native, untagged FocA, for example, in strain DH702 (Figure S2b). In order to demonstrate that FocAΔK2-P31 was indeed synthesized, *focA* gene expression was induced with anhydrotetracycline (AHT) and analysis of membrane fractions

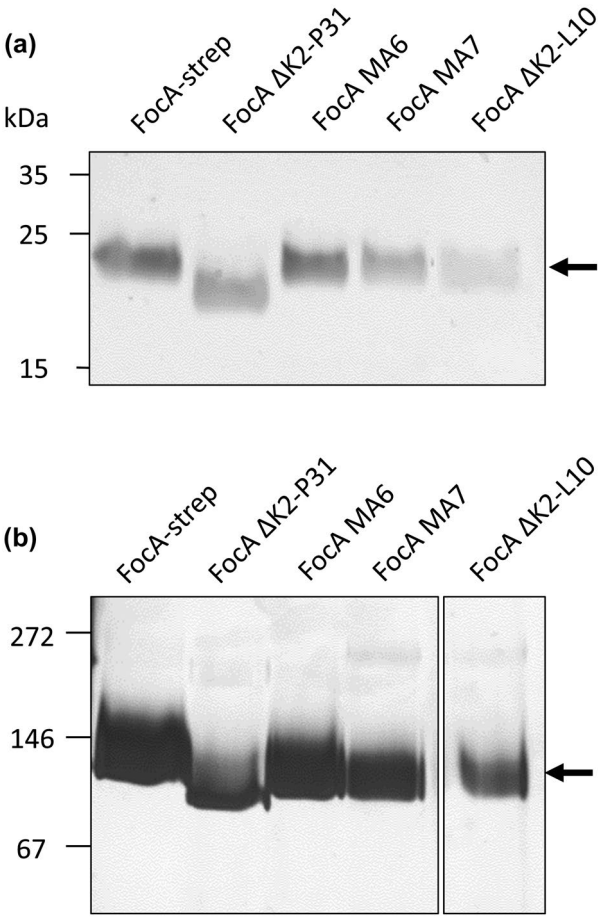

FIGURE 3 Both the amino acid-exchange variants and truncated derivatives in the N-terminal domain of FocA form homopentamers. (a) Shown is a silver-stained SDS-PAGE (12.5% w/v polyacrylamide) in which the indicated purified FocA variants (1 μg of protein) were electrophoretically separated. The migration position of a FocA monomer is displayed on the right with an arrow and migration positions of molecular mass markers (PageRuler Prestained Protein Ladder, Thermo Fisher Scientific) in kDa are indicated on the left of the figure. (b) The same purified FocA variants (1 μg of protein) were separated in BN-PAGE employing a 4%–16% (w/v) polyacrylamide gradient. After electrophoretic separation, the gel was silver-stained and the migration position of a FocA pentamer (~140 kDa) is indicated with an arrow on the right and the migration positions of molecular mass markers (Serva) are shown on the left. The native markers include jack bean urease (272 kDa), porcine lactate dehydrogenase (146 kDa), and bovine serum albumin (67 kDa)

from these cells by western blotting revealed clearly the presence of FocAΔK2-P31 (Figure S2a). As a further control, we determined β-galactosidase enzyme activity of DH701/pfocAΔK2-P31 with and without AHT treatment and could show that even after strongly enhanced synthesis of the truncation derivative, no significant change in β-galactosidase activity compared with the *focA* mutant DH701 was detected in the presence of AHT (Figure S3a). In the absence of AHT, β-galactosidase enzyme activity of strain DH701/pfocAΔK2-P31 increased approximately 40% when compared with DH701 (*focA*), which presumably was due to the

strongly increased abundance of the protein. Note that these cultures were grown to the early stationary phase and this is why the level of *fdhF*$_p$::*lacZ* gene expression, measured as β-galactosidase enzyme activity, was lower than in exponentially growing cells.

Together, these data demonstrate that the N-terminally truncated variants, when expressed from a plasmid, are synthesized in lower amounts compared with the full length, recombinant protein, but they nevertheless form membrane-integral homopentamers like the native FocA protein.

2.3 | Identification of amino acid residues in the N-terminal domain critical for formate translocation

To facilitate the construction of amino acid variants of FocA, we performed the experiments with C-terminally strep-tagged FocA proteins throughout this study. To demonstrate that addition of a C-terminal strep-tag had no influence on the function of FocA in vivo, we determined β-galactosidase enzyme activity after anaerobic growth of strain DH701 (*focA*) transformed with plasmids encoding native FocA with and without a C-terminal strep-tag, as well as FocAΔK2-P31 with and without a strep-tag, and in no case was any significant effect of the strep-tag on β-galactosidase enzyme activity noted (Figure S3b).

Having determined that FocAΔK2-L10 has a similar phenotype regarding formate translocation as FocAΔK2-P31 in DH701 (see above), we next substituted the amino acid residues 2 through 11 completely with alanyl residues (construct FocAMA10, Figure 1c). This FocA variant was introduced into strain DH701 and β-galactosidase enzyme activity after anaerobic growth in minimal medium with glucose was determined (Figure 4). The results showed that this amino acid variant had an enzyme activity that was around 90% the level of that of the *focA* mutant DH701, indicating that this variant was also impaired in formate efflux, despite having a full-length N-terminal domain (Figure 4).

The alanyl-residue substitutions in this derivative were successively changed back to the respective original amino acid residue (see Figure 1c) and β-galactosidase enzyme activity of DH701 transformed with the cognate plasmid was determined (Figure 4). The results revealed that none could restore β-galactosidase enzyme activity to a level like that of recombinant FocA, with the exception of the FocAMA2 variant, which had a single amino acid substitution of K2A. The variant FocAMA3 (exchanges of K2-D4 to A; Figure 1c) restored approximately 33% less β-galactosidase activity when compared to the level measured for native, recombinant FocA in DH701 (Figure 4). Successive introduction of further alanyl residues resulted in progressive loss of the ability of the protein to efflux formate, and variants MA4 (exchanges of K2-N5 to A) through MA7 (exchanges of K2-D8 to A) were essentially inactive. Surprisingly, however, the FocAMA8 variant, in which residues 2 through 9 were exchanged for Ala, had approximately 50% of the β-galactosidase activity compared with that measured in DH701/pfocA3 (Figure 4). The sinusoidal variation in the activities measured for the different variants suggested that both primary and secondary structural changes might be responsible for these effects. These FocA variants were synthesized and formed pentameric, membrane-integral proteins as shown exemplarily for variants FocAMA6 and FocAMA7 (Figure 3).

Despite lack of a clear consensus sequence in the N-terminal domain of FocA when compared with other FNT proteins (see Figure 1a), with the possible exception of the prolyl residue at amino acid position 12, the alanyl-residue substitution data nonetheless suggested that perturbation of the sequence at the N-terminus of the protein caused a significant impairment of formate-translocation activity. We therefore decided to introduce single amino acid exchanges in potential key residues and constructed FocAD4A, FocAN5A, FocAP6A, and FocAP12A variants (see Figure 1c). After transformation of the cognate plasmid into strain DH701 and anaerobic cultivation, the impact of these exchanges on β-galactosidase enzyme activity was investigated (Figure 4). The D4A substitution reduced the enzyme activity of the variant in DH701 (*focA*) only by approximately 20% compared with

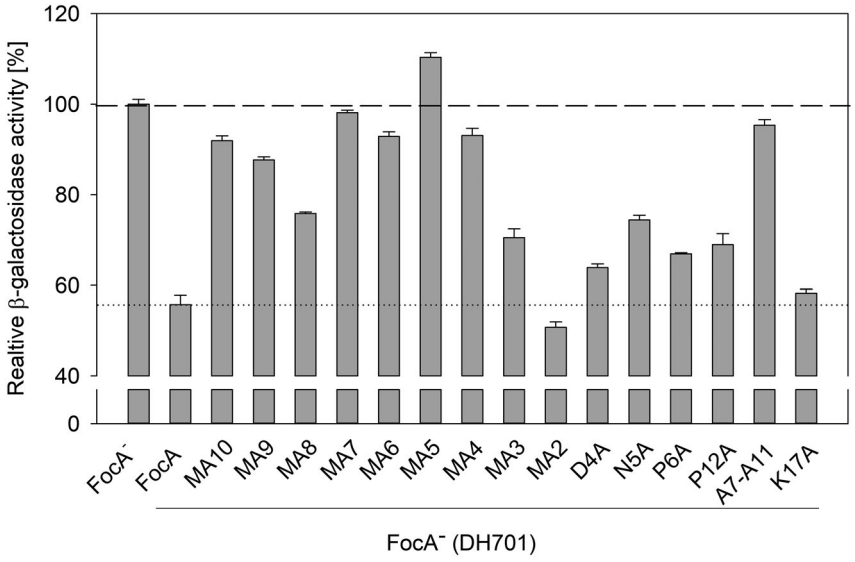

FIGURE 4 Expression of the formate-dependent *fdhF*$_p$::*lacZ* reporter in *focA* mutant DH701 synthesizing various amino acid-exchange variants of FocA. Shown are the relative β-galactosidase enzyme activities of strain DH701 (*focA*) transformed with plasmids carrying genes encoding the indicated FocA derivatives after anaerobic growth in glucose-minimal medium. FocA$^-$ = DH701. The dashed line in the diagram indicates 100% activity, which is equivalent to 616 ± 19 Miller units, while the dotted line signifies the activity determined for DH701 transformed with pfocA3

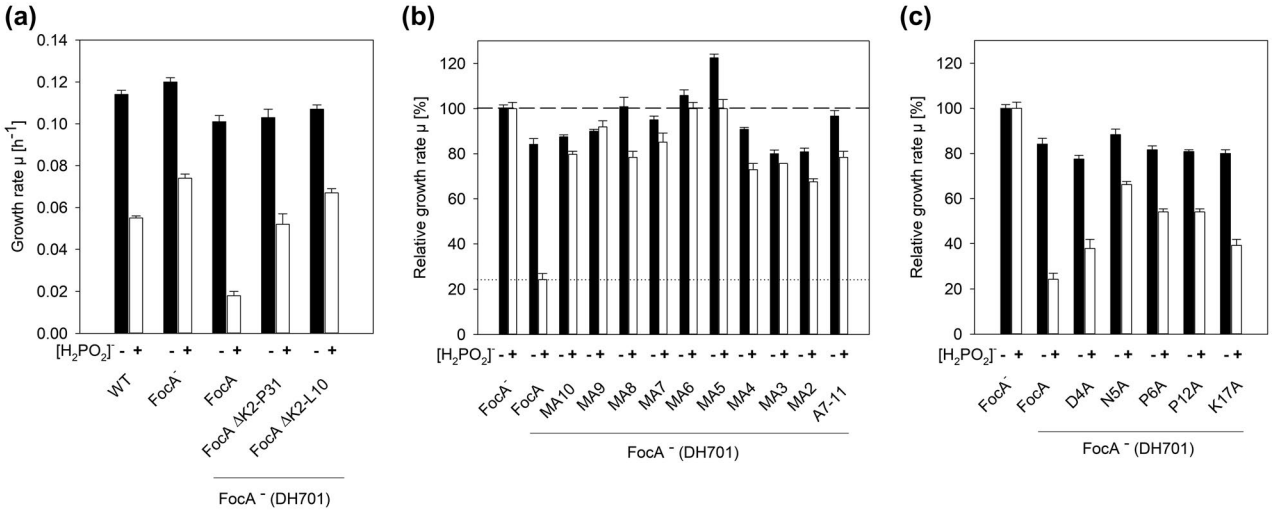

FIGURE 5 Influence of the FocA amino acid-exchange variants on the sensitivity of strain DH701 (*focA*) to the toxic formate analog hypophosphite. Shown are the growth rates (a) or relative growth rates (b, c) of the indicated strains grown anaerobically in glucose-minimal medium in the absence (black bars; "-") or presence (white bars; "+") of 10 mM sodium hypophosphite ($H_2PO_2^-$). WT = DH4100; FocA$^-$ = DH701 (*focA*). The dashed lines in diagrams (b) and (c) indicate the growth rate of DH701 in the absence or presence of hypophosphite: the 100% value in the absence of hypophosphite was $\mu = 0.12 \pm 0.002\ h^{-1}$, while that in the presence of hypophosphite was $\mu = 0.074 \pm 0.002\ h^{-1}$. The dotted line signifies the lowest growth rate (highest hypophosphite-sensitivity) determined for DH701 transformed with pfocA3

the activity of DH701/pfocA3, indicating that this FocA variant retained the ability to allow formate efflux (Figure 4). Exchanging N5 for alanine resulted in a 42% reduction in β-galactosidase enzyme activity relative to native FocA (DH701/pfocA3), while exchanging either P6 or P12 with alanine resulted in a 25%–30% reduction in β-galactosidase enzyme activity, similar to what was observed for the D4A variant of FocA. As a control we also made the K17A exchange, which is located closer to the TM1 junction, and this variant had a β-galactosidase enzyme activity similar to that of the native FocA protein (Figure 4). These data suggest that, although the asparaginyl residue at position 5 (see Figure 1c), near the N-terminus of the soluble cytoplasmic domain has an important role in conferring the ability of the protein to translocate formate out of the *E. coli* cell, it appears that the secondary structure of this domain might have a significant impact on formate efflux. In support of this, when we substituted the residues F7 through L11 with a penta-alanine tract (variant FocAA7-A11) and analyzed *fdh-F*$_p$::*lacZ* expression, β-galactosidase enzyme activity was lowered only by approximately 5% compared with the activity level in the *focA* mutant DH701, strongly suggesting that the structure of this region of the N-terminal domain is also clearly important for FocA function in the formate-efflux direction.

2.4 | The N-terminal domain is critical for uptake of the toxic formate analog hypophosphite

The chemical analog of formate, hypophosphite, is toxic to anaerobically growing *E. coli* and one of its targets is the active PflB enzyme (Plaga et al., 1988). One main route by which hypophosphite enters the anaerobic *E. coli* cell is via FocA, as evidenced by the fact that *focA* mutants exhibit enhanced resistance to hypophosphite (Hunger et al., 2017; Suppmann & Sawers, 1994). Because hypophosphite uptake impairs anaerobic growth of *E. coli*, this can be used as a proxy to examine the effect of the amino acid residue exchanges in FocA on the efficacy of hypophosphite uptake. When strain DH701 (*focA*) was grown anaerobically with glucose, and either without or with 10 mM hypophosphite, an approximately 40% reduction in growth rate was recorded (Figure 5a). A similar experiment carried out with strain DH701 transformed with pfocA3 revealed that the presence of recombinant FocA caused an approximate 80% reduction in the growth rate when hypophosphite was added to the growth medium (Figure 5a). Introduction of plasmids pfocAΔK2-L10 or pfocAΔK2-P31 into DH701 resulted in a hypophosphite-sensitivity similar to the *focA* mutant DH701, indicating that these FocA variants were impaired in hypophosphite uptake into the cell.

Addition of hypophosphite to the anaerobic cultures of DH701 synthesizing FocA variants with multiple, successive substitutions of alanyl residues at the N-terminus of FocA all exhibited sensitivity to hypophosphite, which ranged from 40% (FocA variant M9A, like the *focA* mutant, DH701), to maximally 53% reduction in growth rate (FocA variant M8A). The native, recombinant FocA showed an approximate 82% reduction in growth rate (Figure 5b, Table S1). Unexpectedly, the FocAMA2 variant, with an alanyl-residue substituting K2 (Figure 1c), showed a sensitivity of approximately 50%. This contrasted the near wild-type β-galactosidase activity of the same construct in the formate-efflux direction (compare Figure 4). This suggests a distinction in efflux and influx capabilities of this FocA variant.

Finally, the single amino acid substitution variants, including D4A, N5A, P6A, and P12A, all showed only partial sensitivity to hypophosphite (Figure 5c, Table S1), which correlates with the defects observed in formate translocation out of the cell for the respective variants (cf. Figure 4).

2.5 | Formate import by FocA variants—Impact of inactive PflB

To analyze formate uptake using the *fdhF*$_P$::*lacZ* assay in strains synthesizing the different FocA variants, a mutant derivative of DH701 was constructed in which the gene specifying PflB activase, *pflA*, was deleted (see Experimental procedures). Strain DH601 (*focA* Δ*pflA fdhF*$_P$::*lacZ*) (Table S1) thus lacks FocA, but retains the ability to synthesize the inactive PflB and TdcE enzymes species. Consequently, the strain cannot generate formate from pyruvate, although the inactive glycyl-radical enzymes are made. Growth of DH601 anaerobically in the presence of glucose yielded a β-galactosidase enzyme activity of less than 10 Miller units, while anaerobic growth of DH601 in the presence of glucose and 20 mM formate yielded a β-galactosidase enzyme activity of approximately 1,200 units (Figure 6). As mentioned above, in the absence of FocA, formate can still enter the anaerobic cell through minimally one other, as yet unidentified, uptake system (Rossmann et al., 1991; Suppmann & Sawers, 1994). Transformation of plasmid pfocA3, encoding native FocA, into DH601 increased β-galactosidase enzyme activity by around 50% after anaerobic growth in the presence of 20 mM formate. This result demonstrates that FocA can enhance uptake of formate into anaerobic cells during growth (Figure 6). Introduction of plasmid pfocAΔK2-L10 into DH601 failed to result in enhanced formate-dependent β-galactosidase enzyme activity, which indicates that formate import via FocA is also dependent on the soluble cytoplasmic domain of the protein (Figure 6); a similar result was obtained with DH601/pfocAΔK2-P31 (Figure 6).

Analysis of the sensitivity toward hypophosphite of strain DH601 synthesizing these variants of FocA revealed that, while anaerobic growth of DH601 was unimpaired in the presence of 10 mM sodium hypophosphite, due to the fact that PflB was inactive, and therefore, no longer a target for hypophosphite, introduction of the wild

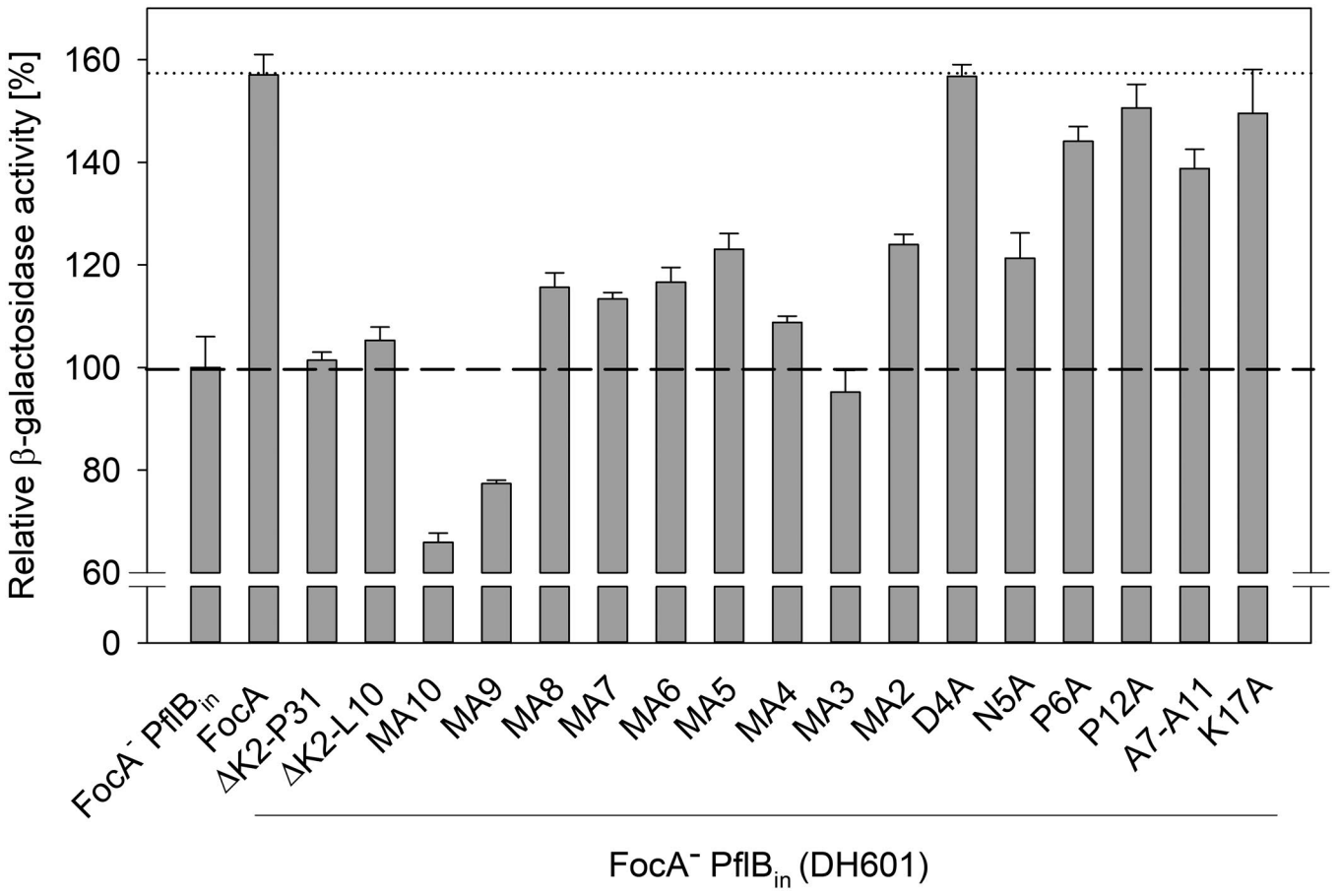

FIGURE 6 Effect of inactivation of PflB on formate-dependent *fdhF*$_P$::*lacZ* reporter expression in a *focA* mutant synthesizing various FocA amino acid-exchange variants. Shown are the relative β-galactosidase enzyme activities of strain DH601 (*focA*, *ΔpflA*), indicated as FocA$^-$-PflB$_{in}$ (inactive PflB) transformed with plasmids carrying genes encoding the indicated FocA variants after anaerobic growth in glucose-minimal medium supplemented with 20 mM sodium formate. The dashed line in the diagram indicates 100% activity of strain DH601 (1,180 ± 70 Miller units), while the dotted line signifies the activity determined for DH601 transformed with pfocA3

type, recombinant *focA* gene on pfocA3 resulted in an approximate 65% decrease in the growth rate (i.e., increased sensitivity) in the presence of the formate analog (Figure 6). This result suggests that FocA takes up hypophosphite at a sufficient concentration for the anion to be able to target a further, unidentified hypophosphite-sensitive enzyme activity in anaerobically growing *E. coli*. Notably, both N-terminal truncation derivatives of FocA were resistant to hypophosphite, indicating that without a complete N-terminal domain, the protein is unable to translocate either hypophosphite or formate into the cell.

Introduction of the poly-alanine tract from residue 2 through 11 into FocA (FocAMA10, Figure 1c) resulted in a β-galactosidase enzyme activity that was 35% lower than that of the original strain DH601 lacking FocA (Figure 6). This unexpected result suggests that this FocA variant is not only unable to import formate, but also appears to have an enhanced efflux capability in this genetic background. Strikingly, a similar activity was observed for FocAMA9 (Figure 6). Both variants showed a low formate-efflux capability when synthesized in DH701, which has an active form of PflB (cf. Figure 4). Residual β-galactosidase enzyme activity, amounting to roughly 25% of the wild-type level, was measured for derivatives FocAMA8 through FocAMA5 and for FocAMA2, while FocAMA4 and FocAMA3 were inactive. Together with the observation that the FocAD4A single amino acid substitution variant showed wild-type β-galactosidase activity (Figure 6), these findings indicate that amino acid residue K2 is important for formate uptake when PflB is in its inactive form. The P6A, P12A, and K17A exchange variants of FocA also exhibited wild-type or near wild-type β-galactosidase enzyme activity (Figure 6), suggesting unimpaired formate import capacity. Only the FocAN5A variant had a clearly reduced β-galactosidase activity, again emphasizing the importance of this residue for FocA function.

Remarkably, exchange of the residues 7 through 11 with a penta-alanine tract did not abolish formate import activity, with a retention of approximately 67% of the wild-type activity (Figure 6). This result indicates that the KADNP motif between residues 2 and 6, in particular residue N5, in the N-terminal domain is important for formate influx in DH601 (PflB is in its inactive form). This motif is, however, insufficient on its own to facilitate formate efflux when PflB is active (in strain DH701), and in this case the leucyl residues at positions 10 and 11 also appear to be important. Together, these results indicate that in a strain synthesizing inactive PflB, the N-terminal residues K2 and N5 are both particularly important for formate uptake by FocA. However, they seem to play a less important, secondary, role in formate efflux. Thus, conformational organization of this region appears to have an overriding effect when PflB is in its enzymatically active state. Moreover, these results clearly indicate a difference in mechanism between efflux and influx of formate.

Analysis of the sensitivity toward hypophosphite of DH601 synthesizing the different variants of FocA revealed that, while anaerobic growth of DH601 was essentially unaffected by the presence of 10 mM sodium hypophosphite, introduction of the wild-type *focA* gene restored clear sensitivity toward the formate analog (Figure S4). Notably, both of the N-terminal truncation variants of FocA, as well as all poly-alanine substitution variants were resistant to hypophosphite, which indicates hypophosphite is not imported and more or less reflects the findings with regard to formate uptake. On the contrary, the D4A, P6A, P12A, and K17A variants all showed wild-type sensitivity to hypophosphite (Figure S4). Remarkably, however, the FocAA7-A11 variant was also strongly impaired in hypophosphite uptake, which contrasts the ability of this derivative to perform formate influx. This suggests that the residues between F7 and L11, and their impact on the overall structure of FocA´s N-terminal domain, play a decisive role in hypophosphite uptake but are less crucial for formate uptake. The effects of hypophosphite on growth of DH701 and DH601 synthesizing the different FocA variants are summarized in Table S1.

2.6 | Influence of amino acid exchanges in the N-terminal domain of FocA in a strain completely lacking PflB

Several of the amino acid-exchange variants were also tested for their ability to translocate formate into a strain that lacked the gene encoding PflB, strain DH201 Δ(*focA pflB*) (Figure S5; Sawers & Böck, 1988). This strain was tested because it lacks PflB and, because previous results revealed that PflB can interact with the N-terminal domain of FocA (Doberenz et al., 2014), we wished to determine whether there was a difference in formate uptake between a strain that has no PflB enzyme and one that synthesizes an inactive PflB enzyme. Truncation of, or introduction of poly-alanyl residues into, the N-terminal domain of FocA inactivated the protein with respect to formate import activity. In contrast, the variant FocAD4A (exchange of Asp at position 4 to Ala), when introduced into DH201, caused an approximate 125% increase in β-galactosidase enzyme activity when compared with the activity of the original strain DH201 (Δ*focA* Δ*pflB*) (Figure S5). A similar increase in β-galactosidase enzyme activity was measured when pfocA3 was introduced into DH201 and this activity was also similar to that determined for the *E. coli* parental strain DH4100 (Figure S5). Exchanging the asparaginyl residue at position 5 for an alanyl residue (variant FocAN5A in Figure 1c) resulted in a β-galactosidase enzyme activity that was 25% lower than that of strain DH201 (Figure S5). This suggests not only that this FocA variant is impaired in formate uptake, but also that in the absence of PflB, this FocA variant preferentially translocates formate out of the cell. Moreover, while the P6A variant retained 45% of the formate influx capability when compared with native, recombinant FocA (DH201/pfocA3), the P12A FocA variant had an activity phenotype like that of the N5A variant (Figure S5). Together, these data indicate that despite the absence of PflB in strain DH201, native, recombinant FocA can still take up formate; however, this uptake is still dependent on the N-terminal domain. Furthermore, all amino acid residue exchanges in the N-terminal domain, except Asp at position

4, resulted in loss of formate uptake capability, while exchanges of the N5 and P12 residues resulted in even lower β-galactosidase enzyme activity than the original strain, suggesting increased efflux of formate. These results are consistent with active and inactive forms of PflB, and possibly also TdcE (Falke et al., 2016), having a role in regulating formate translocation through FocA.

3 | DISCUSSION

The apparent lack of conservation, both in length and amino acid sequence, of the soluble N-terminal domain is a striking feature within the FNT channel family (Figure 1a). Even when the N-terminal domain from FocA proteins within key genera of proteobacteria and Gram-positives are compared, this also reveals considerable variation in amino acid sequence conservation and domain length, the exception being the prolyl residue at amino acid position 12 in the first half of the domain in *E. coli* FocA (Figure S6). The general lack of conservation notwithstanding, the results of this study provide the first insights into the importance of this soluble N-terminal domain in modulating bidirectional formate permeation through the FocA pentamer's pores. Defining the precise length of the N-terminal domain of FNT proteins is made more difficult by the often poorly defined structure of the soluble domain (Wang et al., 2009). However, structural analysis of the well-defined α-helical N-terminal domain of the hydrosulfide ion channel HSC of *C. difficile* (Czyzewski & Wang, 2012) helped pinpoint the first amino acid of the TM1 helix in FocA to be near Leu31 (Figure 1a). Removal of this 31 amino acid residue long N-terminal domain of FocA revealed that it is essential to allow formate to pass through the pore, in either direction. Although no function has yet been ascribed to the soluble N-terminal domain of any FNT protein, structural analysis of several of these proteins has suggested that this domain might have a role in providing a support that moves TM2b and the associated Ω-loop into the cytoplasmic vestibule, consequently closing the pore (Czyzewski & Wang, 2012; Lü et al., 2011; Waight et al., 2013). The observation that diffracting crystals of *E. coli* FocA could only be obtained after removal of the first 22 amino acid residues of the N-terminal domain, and that all pores within the structure that was ultimately obtained were in the closed conformation (Wang et al., 2009), supports the hypothesis that the N-terminal domain might function to modulate pore access. A further FocA structure was subsequently obtained with a full-length protein (Lü et al., 2011) and revealed a mix of open and closed pores, which had different orientations of the N-terminal domain. These structural analyses support the proposed function of the N-terminal domain in "gating" the channel within FNT proteins by controlling the position of the associated Ω-loop (Figure 1b). Analysis of the N-terminal amino acid residue-exchange variants of FocA constructed in this study, which do not perturb the domain's length, clearly demonstrates that both the secondary structure and certain amino acid residues of this soluble domain have key biochemical functions in vivo, possibly even directly controlling the direction of formate permeation. The question that remains to be addressed in future studies is how this biochemical control is achieved.

The truncation variant of FocA lacking the complete N-terminal domain could be purified from the membrane fraction and was shown to form pentamers. Nevertheless, it was clearly synthesized in lower amounts than the native, full-length protein. This is reminiscent of the consequence of truncation of the C-terminus of FocA on membrane integration (Hunger et al., 2017), particularly when the truncation impinged upon the integrity of the TM, and suggests that the removal of key hydrophilic residues prevents the helix being stably anchored within the membrane. Nonetheless, because a similar phenotype, with respect to impaired formate permeation, was also observed when only the first 10 N-terminal amino acids residues of FocA were removed, this might actually suggest that certain sequence requirements govern or affect either protein synthesis or turnover, membrane-insertion, or indeed the function of the protein, and thus, cause lowering of its stability when they are removed.

To obviate the potential destabilization of FocA by decreasing the length of the N-terminal domain, we decided initially to replace the missing amino acid residues from positions 2 to 11 with a poly-alanine tract. The length of this protein was thus similar to the native protein but, although readily purified, it also exhibited reduced levels in the membrane. Most importantly, however, this protein was also inactive in bidirectional formate permeation. Only when almost all of the original amino acid residues were restored, could formate efflux by the FocA variant be recovered. Using a combination of experimental and molecular biological approaches, we could show that a motif (KADNP) at the immediate N-terminus (Figure 1b) of FocA appears to be important for the ability of the *E. coli* protein to permeate formate bidirectionally; the asparaginyl residue at position 5 is particularly important. However, our data also suggest that the overall structure of the N-terminal domain appears to be important for FocA function in vivo.

Using the Pep-fold algorithm it can be predicted that the first 36 N-terminal amino acids of *E. coli* FocA fold to form two short α-helices separated by a loop, and with a flexible N-terminus (Figure 7); a superposition of four structural models for this domain are shown in Figure S7. It is clear from these conformational predictions that the N-terminal domain is highly flexible, which is in agreement with earlier findings (Wang et al., 2009). Changing the residues from position 2 to 11 to alanines (FocAM10A) causes complete distortion of the predicted structure of the domain and significantly alters the orientation of the N-terminal amino acids (Figure 7b), which correlates with loss of formate-translocation capacity of the FocAMA10 variant. Structural predictions performed using the Pep-fold algorithm of the other N-terminal variants emphasizes how small sequence changes can have a significant effect on the predicted secondary structure of the domain (Figure S8), which again correlates with the significant effects observed for these proteins on formate efflux and influx. Whether these hypothetical structural changes effect changes in the position of the Ω-loop or interaction with PflB will require further detailed study. Notably, reintroduction of the KADNP residues to the poly-alanyl variant restores the helices to the predicted structure (Figure 7b), and this also correlates with recovery of the ability of the variant to take up formate (see Figure 6). However, this does not explain why translocation

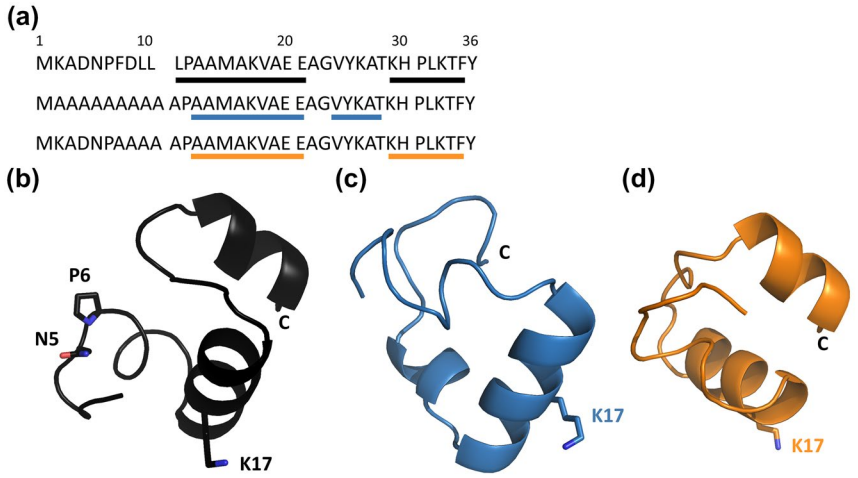

FIGURE 7 Comparison of a selection of predicted conformational models of the N-terminal domain of FocA. (a) The amino acid sequence of the first 36 residues of wild-type FocA (top), the FocAMA10 variant (middle), and FocAA7-L11 variant (bottom) are aligned. The bars below each sequence indicate locations of α-helical structure in the respective domains, as predicted using the Pep-fold 3.5 algorithm. (b). The predicted structural model of the 36 amino acid-long N-terminal sequence of wild-type FocA is shown. Those for FocAMA10 (c) and FocAA7-L11 (d) are displayed side-by-side. In each structural representation the C-terminal portion of the peptide was fixed in the upper right-hand quadrant of the depiction. Amino acid residues N5, P6, and K17 are shown for orientation purposes. The colors correlate with the sequences in part A

of formate functions only in the influx direction and only when PflB is inactive (cf. Figures 4 and 6).

3.1 | How might the N-terminal domain function to gate the FocA pore?

A recent cryo-electron microscopy-based structural analysis of a calcium-gated potassium channel (Fan et al., 2020) demonstrated that when its N-terminal domain was truncated, the pore retained a permanently "open" conformation and could not be inactivated. This supported a "ball-and-chain"-type mechanism for gating of the pore cavity, originally suggested in earlier studies (Hoshi et al., 1990; Zagotta et al., 1990), and which the authors suggest is governed by calcium binding to the soluble domain. The difference in gating mechanism between the Shaker cation channel and the FocA anion channel is that in the former the N-terminal domain is required to inactivate the channel, while in the latter, the N-terminal domain is required to activate the channel. In FocA, there is currently no evidence to suggest that the N-terminal domain might bind a small molecule. We have, however, shown in earlier studies that FocA interacts with the glycyl-radical enzymes PflB and TdcE (Doberenz et al., 2014; Falke et al., 2016), both of which are formate-producing enzymes. Notably, chemical cross-linking and modeling studies identified numerous interactions between PflB and the N-terminal domain of FocA (Doberenz et al., 2014). It is conceivable, therefore, that PflB and/or TdcE interact with FocA in vivo to facilitate "gating" of the pores of FocA. This would invoke a type of "spring-" or "lever-type" mechanism, whereby the binding of the interacting protein would cause the N-terminal domain to allow the TM2b-Ω-loop to move out of the pore by breaking the hydrogen-bond between His-209 and Thr-91 (*E. coli* FocA numbering), which, based on structural analyses, has been suggested previously as a possible mechanism controlling opening of the substrate pore (Waight et al., 2013; see also the model in Figure 1b). Such a mechanism would also be in accord with the closed-pore conformation of the FocA structure in which the N-terminal domain was missing (Wang et al., 2009). Although speculative at this stage, this working hypothesis provides a basis for future experiments to address the biochemical mechanism underlying the function of the N-terminal domain.

It is perhaps noteworthy that there were differences in the formate-translocation activity for key amino acid variants, particularly FocAA7-A11 (penta-alanyl tract from positions 7 to 11), depending on whether PflB was in its inactive or active conformation; formate influx was functional but efflux was impaired (see Figures 4 and 6). It has long been proposed that PflB has a significantly different conformation when the glycyl radical is present in the enzyme compared to when it is not (Knappe & Sawers, 1990) and evidence supporting such a conformational change has been reported (Peng et al., 2010). It seems likely, therefore, that, depending upon whether PflB is in its glycyl-radical-bearing conformation, a different interaction with FocA occurs compared to when PflB is inactive and this might potentially govern or influence "gating." It is conceivable, for example, that formate efflux occurs during growth when PflB is active, while influx occurs when growth stops and PflB is in its inactive conformation (Beyer et al., 2013; Suppmann & Sawers, 1994). In the absence of PflB (e.g., strain DH201), it is possible that the glycyl-radical enzyme TdcE could take over this function (Sawers et al., 1998) and in its active conformation would block formate influx, which is what was observed in the current study when DH201 synthesizes FocAA7-A11 (Figure S6). TdcE, like PflB, has been shown in vitro to interact with FocA (Falke et al., 2016). Of course, the pH shift that occurs upon entry into stationary phase under these growth conditions (see Suppmann & Sawers, 1994) must also be

considered to play a role in protonation of the His-209 residue in the substrate pore of FocA (Lü et al., 2013; Waight et al., 2013).

3.2 | Formate efflux and influx mechanisms are different

FocA was originally suggested to function as a channel for efflux of either formate or undissociated formic acid (Suppmann & Sawers, 1994). Proton-coupled formate efflux would be highly beneficial for an energy-limited fermenting bacterium and recent computational studies support such a proton-anion symport mechanism (Atkovska & Hub, 2017; Lv et al., 2013). This implies, however, that formate uptake is also likely to be via a proton-symport mechanism, suggesting involvement of the proton gradient. Heterologous expression studies of FocA support pH- and proton-driven formate uptake into yeast cells (Wiechert & Beitz, 2017). However, in the homologous *E. coli* system, in cells unable to metabolize formate intracellularly due to a *selC* mutation that prevents selenocysteine incorporation into formate dehydrogenases (Leinfelder et al., 1988), no formate uptake occurs (Beyer et al., 2013). This implies a specific gating mechanism to control formate uptake and not a simple *pmf*-driven proton symport, which would otherwise result in intracellular accumulation of formate. The findings presented in this study indicate that the N-terminal domain of FocA is involved in gating formate influx. Moreover, through the study of sensitivity toward the toxic formate analog hypophosphite, our data also suggest that not only the mechanisms of formate efflux and uptake differ, but also the uptake mechanisms of hypophosphite and formate may exhibit differences. For example, the FocAA7-A11 variant is capable of formate uptake but cells remain resistant to hypophosphite (cf. Figures 6 and S4). The pK_a of formate is 3.75 while that of hypophosphite is 1.1, suggesting that differences in how readily the anion can be protonated has a major impact on influx; nevertheless, the wild-type FocA protein can import both anions. These similarities and differences in anion preference between formate and hypophosphite will be invaluable in future experiments designed to dissect the influx mechanism of the FocA channel.

4 | EXPERIMENTAL PROCEDURES

4.1 | Strains and growth conditions

The bacterial strains and plasmids used in this study are listed in Table S2. Preparation of aerobic cultures of *E. coli* for molecular biology experiments was performed in Luria–Bertani (LB) medium (Sambrook et al., 1989). Growth of strains for analysis of β-galactosidase enzyme activity, for determination of formate levels excreted into the growth medium, for hypophosphite-sensitivity analysis, or for preparation of membrane fractions was performed in M9-minimal medium (Sambrook et al., 1989), which included 47.6 mM Na_2HPO_4, 22 mM KH_2PO_4, 8.4 mM NaCl, 20 mM NH_4Cl, 2 mM $MgSO_4$, 0.1 mM $CaCl_2$, 0.1 mM thiamin dichloride, 1 mM trace element solution (Hormann & Andreesen, 1989), and 0.8% (w/v) glucose as carbon source. Growth of BL21(DE3) strains carrying appropriate Strep-tagged FocA variants for protein purification was done in TB medium, which included 1.2% (w/v) tryptone, 2.4% (w/v) yeast extract, 0.4% (w/v) glycerol, 0.8% (w/v) glucose, 100 mM potassium phosphate, and pH 7 as described (Doberenz et al., 2014; Hunger et al., 2014). Where indicated, sodium formate was added to a final concentration of 20 mM. When required, antibiotics were used at a final concentration of 12.5 μg/ml for chloramphenicol, 50 μg/ml for kanamycin, and 125 μg/ml for ampicillin.

4.2 | Hypophosphite-sensitivity test

The sensitivity of strains transformed with plasmids encoding various FocA variants toward the formate analog hypophosphite was tested by growing strains anaerobically at 37°C in M9 minimal medium containing 0.8% (w/v) glucose and 10 mM sodium hypophosphite. The growth rates of exponential phase cultures were compared after cell growth with and without added hypophosphite. Growth was followed by measuring the optical density at 600 nm of standing liquid cultures (0.2 ml) in microtiter plates using a Tecan Infinite M Nano (Tecan, Germany) spectrophotometer. Experiments were performed in triplicate and growth rates are presented with standard deviation of the mean.

4.3 | Construction of strains and plasmids

In order to construct the strain DH601, a derivative of MC4100 (Casadaban, 1976; MC4100 *focA*, Δ*act* Ω(*act*::*cat* pACYC184), $fdhF_p$::*lacZ*), the respective Δ*pflA* allele was transduced into strain REK701 (*focA*) (Suppmann & Sawers, 1994) using $P1_{kc}$-mediated transduction with the phage grown on strain 234M1 (MC4100 Δ*act* Ω(*act*::*cat* pACYC184); Wagner et al., 1992), according to the procedure described (Miller, 1972). The correct integration of the chloramphenicol resistance cassette into *pflA* without reintroducing the wild-type *focA* gene was verified by colony PCR using oligonucleotides 5′-CTAAACTGCCGTTTGCTTACG-3′ and 5′-GATGTGTTA AAAACGCTGTAGCAGAATGAAGC-3′. Moreover, the presence of the *focA* mutation was verified by PCR using the oligonucleotides 5′-CTGTTTTAGCGGAGGATGCG-3′ and 5′-GTTTGCGATACTGAA CGCAAAACCG-3′. Finally, MC4100 *focA act*::Cm^r was transduced with λ($fdhF_p$::*lacZ*) (Falke et al., 2010), delivering DH601.

The construction of plasmids carrying *focA* genes encoding N-terminal FocA variants was achieved using expression plasmid pfocA3 (Falke et al., 2010) as template, either for site-directed mutagenesis (Agilent Technologies) or for PCR of truncated *focA* fragments, which were subcloned into the pASK-IBA3 (IBA Lifesciences, Göttingen) via BsaI restriction sites. Oligonucleotides used for the cloning or mutagenesis methods, and their respective templates if these were not pfocA3, are listed in Table S3. The plasmids encoding variants of FocA were transformed into the indicated strains, which

are listed in Table S2, carrying a chromosomal λ *fdhF*$_P$::*lacZ* transcriptional fusion (Falke et al., 2010).

4.4 | Preparation of cell extracts and membrane fractions

In order to determine levels of FocA associated with the membrane fraction, cells were grown anaerobically in 1L cultures in M9-glucose medium, exactly as was done when measuring β-galactosidase enzyme activity (see below). To achieve overproduction of selected FocA variants, gene expression of pASK-IBA3 derivatives was induced by addition of 0.2 mg/L anhydrotetracycline (AHT) when the culture attained an $OD_{600\ nm}$ of approximately 0.4. Incubation of the culture was continued until an $OD_{600\ nm}$ of approximately 1.2–1.6 was reached. Cells were harvested by centrifugation at 4,250*g* for 20 min and at 4°C and afterward the cell pellet was suspended in 4 ml of 50 mM Tris-HCl, pH 8 including 170 mM NaCl and 2 mM $MgSO_4$ per g wet cell mass. DNase I (10 mg/ml) and 4 mM phenylmethylsulfonyl fluoride (PMSF) were then added and the mixture was incubated for 30 min at 37°C. Cells were disrupted by sonication (25 W for three times 4 min with 0.5 s pulses) on ice. Unbroken cells and cell debris were removed by centrifugation for 45 min at 25,000*g* and at 4°C. The crude cell extract was used to obtain membrane fractions, which were prepared by ultracentrifugation at 100,000*g* for 1 hr and at 4°C (Hunger et al., 2014). The supernatant was collected for the determination of PflB levels in the different strains. The membrane vesicles were suspended in 100 mM Tris-HCl, pH 8.0, 150 mM NaCl, 1 mM EDTA, 16 mM *n*-Dodecyl-*β*-D-Maltoside (DDM from Glycon Biochemicals, Luckenwalde, Germany), and the proteins were solubilized at 4°C by overnight incubation. The protein concentration of the solubilized membrane fraction and soluble cytoplasmic fractions was determined (Lowry et al., 1951) using bovine serum albumin as the standard.

4.5 | Overproduction and purification of strep-FocA and variants

For overproduction of FocA variants carrying a C-terminal strep-tag, cultures of *E. coli* BL21(DE3) containing pfocA3 or the appropriate pfocA3 variant were grown aerobically at 37°C in 0.4 L of TB medium (Soboh et al., 2012) supplemented with 125 mg/L ampicillin to an $OD_{600\ nm}$ of approximately 0.4. Gene expression was induced by addition of 0.2 mg/L AHT and cultures were incubated at 30°C with continuous shaking for a further 18 hr. Cells were harvested by centrifugation as described above and suspended in 20 ml of 50 mM Tris-HCl, pH 8.0, 170 mM NaCl, 2 mM $MgSO_4$ containing DNase I (10 mg/ml) and 4 mM PMSF. After a brief incubation at 37°C, cells were disrupted by sonication at 4°C and the crude cell extract and membrane fraction were prepared as described above.

To solubilize FocA from the membrane, the membrane pellet was suspended in 5 ml of 100 mM Tris-HCl, pH 8.0, 150 mM NaCl, 1 mM EDTA, 16 mM DDM, and the mixture was incubated overnight at 4°C. The solution was subsequently centrifuged for 1 hr at 100,000*g* and at 4°C. The resulting supernatant containing solubilized strep-tagged FocA, or its variants, was supplemented with 3 nM avidin, incubated on ice for 30 min and was then loaded onto a 1 ml column containing 1 ml of Strep-Tactin-Sepharose matrix (IBA Lifesciences, Göttingen). Further purification steps were carried out aerobically and at 4°C, exactly as described in the manufacturer's instructions. The yield of FocA-C-strep and its variants generally was in the range of 0.2–0.6 mg/L of culture. The protein concentration of the strep-tagged FocA variants was determined spectrophotometrically, via absorbance at 280 nm with the calculated extinction coefficients (online ProtParam; Gasteiger et al., 2005).

4.6 | Polyacrylamide gel electrophoresis (PAGE) and immunoblotting

Aliquots of 1 μg of the various purified FocA variants were electrophoretically separated in sodium dodecyl sulfate (SDS)-PAGE including 12.5% (w/v) polyacrylamide (Laemmli, 1970) and subsequently transferred to nitrocellulose membranes as described (Towbin et al., 1979). Affinity-purified antibodies directed against full-length FocA were prepared by covalently linking purified full-length FocA to AminoLink sepharose (Thermo Fisher) and the bound antibodies were eluted exactly according to the manufacturer's instructions. Antibodies were used at a dilution of 1:1,000 (Falke et al., 2010). The secondary antibody conjugated to horseradish peroxidase (Bio-Rad, Munich, Germany) was used according to the manufacturer's instructions. Visualization of the antibody–antigen interaction was achieved using the enhanced chemiluminescence reaction using the enhancer *para*-coumaric acid (Haan & Behrmann, 2007).

Blue-native (BN)-PAGE with 1 μg of the various purified FocA variants was performed with 4%–16% gradient gels according to (Schagger & von Jagow, 1991) as described (Falke et al., 2010).

For the detection of FocA variants in the solubilized membrane fractions, samples of 100 μg with respect to protein were separated by gel electrophoresis using either 12.5% (w/v) sodium dodecyl sulfate (SDS) gels or in 16% Tris-tricine gels (Schagger & von Jagow, 1987). To analyze the corresponding PflB levels, samples (50 μg of protein) of the respective soluble cytoplasmic fractions were separated by SDS-PAGE using a 8% (w/v) polyacrylamide gel. After transfer of the proteins to a nitrocellulose membrane, they were treated with antibodies against full-length FocA (membrane fraction) or antibodies raised against PflB (soluble cytoplasmic proteins). PflB antiserum was used at a dilution of 1:1,000. The detection of the luminescence was performed as described above. Where indicated, silver-staining of SDS- or BN-PAGE gels was performed using the Pierce Silver-staining kit (Thermo Fisher Scientific), as described by the manufacturer.

4.7 | ß-Galactosidase activity assays

The ß-galactosidase enzyme activity was determined and calculated according to Miller (1972) and performed as described in (Falke et al., 2010), but with modifications. Different strains were grown anaerobically in 15 ml Hungate tubes in M9-minimal medium containing 0.8% (w/v) glucose. DH4100, DH701, and DH701 transformed with plasmids encoding FocA variants were grown at 37°C until cultures reached the exponential growth phase ($OD_{600\,nm}$ 0.7 to 0.9), usually within 5 to 8 hr. Unless stated otherwise, all FocA variants carried a C-terminal strepII-tag. DH4100, DH601, DH201, and DH601/DH201 containing pfocA3 variants were grown in M9 medium with 20 mM sodium formate at 30°C and reached an $OD_{600\,nm}$ of ~0.8 after 14 to 24 hr. Once the exponential growth phase had been reached, aliquots (100 µl) of cell suspension were transferred to the wells of a 96-well microtiter plate. Microtiter plates were stored at −20°C until measurements of the kinetics were undertaken. For the ß-galactosidase assay thawed cell suspensions were mixed with 20 µl buffer Z (6.5 mM NaH_2PO_4, 93.5 mM Na_2HPO_4, pH 8, 10 mM KCl, and 1 mM MgSO4) supplemented with 50 mM ß-mercaptoethanol and 0.1% (w/v) SDS. Afterward 40 µl trichloromethane was added, the suspension was mixed thoroughly and incubated at 25°C for 5 min. Afterward, 20 µl of the substrate 4 mg/ml para-nitrophenyl-β-D-glucopyranoside (PNPG, Sigma Aldrich, purity > 98%) in buffer Z, were added resulting in a final concentration of 0.44 mg/ml PNPG and kinetic measurements were started. The absorbance at 420 nm was measured at 25°C for 1 hr using a Tecan Infinite M Nano (Tecan, Germany) spectrophotometer. The ß-galactosidase activity was calculated with the following formula $\beta-\text{galactosidase activity} = \frac{1{,}000\times m}{v\times OD_{600}}$.

where m = the slope of the linear regression of the kinetic data, and v = volume of cells (0.1 ml).

Each experiment was performed with a complete set of strains and with independent biological replicates, and each assay was determined in triplicate, that is, technical replicates. Data sets were performed multiples times and those presented are representative for each strain. The activities determined for the truncated and amino acid-exchange variants in backgrounds DH701, DH601, and DH201 are presented in relation to the value for the respective strain without a plasmid, which was taken as 100%. Note that the ß-galactosidase enzyme activity was similar for the strain without a plasmid and when the same strain carryed an insert-free plasmid (data not shown). The absolute ß-galactosidase activities, given in Miller units (Miller, 1972) and in relative units, are presented with standard deviation of the mean.

4.8 | Analysis of extracellular formate levels

Strains (DH4100, DH701, and DH701 pfocA3 variants) were grown anaerobically in M9 minimal medium with 0.8% (w/v) glucose. Samples were prepared by collecting 1.5 ml of each cell suspension once the $OD_{600\,nm}$ of the culture had reached ~ 0.8 and centrifuging through silicon oil (medium-viscosity, PN200, Roth) at 12,000*g* for 5 min. The supernatant was separated by anion-exchange chromatography on an Aminex HPX-87H column (300 × 7.8 mm, polystyrene-divinylbenzene, 9 µm particle size, and 8% cross linkage) with the Micro-Guard Cation H^+ Refill Cartridge precolumn (polystyrene-divinylbenzene, both columns from Bio-Rad Laboratories) using the high-performance liquid chromatography (HPLC) apparatus (Prominence UFLC; Shimadzu). Organic acids, such as formate, were eluted with 6 mM H_2SO_4 at a flow rate of 0.3 ml/min. The column was heated to 42°C. The amount of formate in the supernatant was quantified by integration of the area of the respective elution peaks, which were monitored at 210 nm and referenced to a calibration curve in the range of 0.1 to 50 mM formate. Formate concentration was determined in triplicate and the amount of extracellular formate is presented with standard deviation of the mean.

4.9 | Computational analysis of FocA's N-terminal domain

The degree of conservation of the first 36 N-terminal amino acids of a sequence alignment of 258 annotated formate/nitrite channels (FNTs) was assessed and displayed using the WebLogo tool (Figure 1a; online version WebLogo 3; Crooks et al., 2004). For the conservation plot where only FocA channels were compared, the N-terminal domains from 100 formate channels originating from different species were aligned and evaluated with WebLogo 3 (Figure S6).

De novo modeling of 3D conformations of FocA´s N-terminus, and variants thereof, was performed by the PEP-FOLD Peptide Structure Prediction Server (online version PEP-FOLD 3.5; Lamiable et al., 2016). The input sequence was the first 36 residues of the native FocA protein or selected FocA variants. Each computational process comprised 200 simulations and the models were sorted based on their sOPEP energy level. The online tool returned the five best structure predictions and the resulting PDB files were loaded into PyMOL (The PyMOL Molecular Graphics System, version 0.99, Schrödinger, LLC) and superpositioned to allow structural comparison.

The PyMOL software was also used to illustrate schematically how formate translocation by FocA might be regulated (Figure 1b). X-ray structures of *E. coli* FocA (pdb 3KCU, Wang et al., 2009) and *E. coli* PflB (pdb 1H18, Becker & Kabsch, 2002) were used to generate figures, and FocA´s N-terminal domain was modeled using PEP-FOLD 3.5 (Lamiable et al., 2016).

ACKNOWLEDGMENTS

We are grateful to Marian Baumbach and Mathias Mende for their help in the initial characterization of the truncated variants of FocA. This work was supported in part by the DFG (GRK 1026) and the region of Saxony-Anhalt.

CONFLICT OF INTEREST

The authors declare that they have no conflict of interest to report.

DATA AVAILABILITY STATEMENT

The data that support the findings of this study are available from the corresponding author upon reasonable request.

ORCID

Robert Gary Sawers https://orcid.org/0000-0003-0862-2683

REFERENCES

Atkovska, K. & Hub, J.S. (2017) Energetics and mechanism of anion permeation across formate-nitrite transporters. *Scientific Reports*, *7*, 12027.

Becker, A. & Kabsch, W. (2002) X-ray structure of pyruvate formate-lyase in complex with pyruvate and CoA. How the enzyme uses the Cys-418 thiyl radical for pyruvate cleavage. *Journal of Biological Chemistry*, *277*, 40036–40042.

Beyer, L., Doberenz, C., Falke, D., Hunger, D., Suppmann, B. & Sawers, R.G. (2013) Coordinating FocA and pyruvate formate-lyase synthesis in *Escherichia coli*: preferential translocation of formate over other mixed-acid fermentation products. *Journal of Bacteriology*, *195*, 1428–1435.

Casadaban, M.J. (1976) Transposition and fusion of the *lac* genes to selected promoters in *Escherichia coli* using bacteriophage lambda and Mu. *Journal of Molecular Biology*, *104*, 541–555.

Crooks, G.E., Hon, G., Chandonia, J. & Brenner, S.E. (2004) WebLogo: a sequence logo. *Genome Research*, *14*, 1188–1190.

Czyzewski, B.K. & Wang, D.N. (2012) Identification and characterization of a bacterial hydrosulphide ion channel. *Nature*, *483*, 494–497.

Doberenz, C., Zorn, M., Falke, D., Nannemann, D., Hunger, D., Beyer, L., *et al.* (2014) Pyruvate formate-lyase interacts directly with the formate channel FocA to regulate formate translocation. *Journal of Molecular Biology*, *426*, 2827–2839.

Erler, H., Ren, B., Gupta, N. & Beitz, E. (2018) The intracellular parasite *Toxoplasma gondii* harbors three druggable FNT-type formate and L-lactate transporters in the plasma membrane. *Journal of Biological Chemistry*, *293*, 17622–17630.

Falke, D., Doberenz, C., Hunger, D. & Sawers, R.G. (2016) The glycyl-radical enzyme 2-ketobutyrate formate-lyase, TdcE, interacts specifically with the formate-translocating FNT-channel protein FocA. *Biochemistry and Biophysics Reports*, *6*, 185–189.

Falke, D., Schulz, K., Doberenz, C., Beyer, L., Lilie, H., Thiemer, B., *et al.* (2010) Unexpected oligomeric structure of the FocA formate channel of *Escherichia coli*: a paradigm for the formate-nitrite transporter family of integral membrane proteins. *FEMS Microbiology Letters*, *303*, 69–75.

Fan, C., Sukomon, N., Flood, E., Rheinberger, J., Allen, T.W. & Nimigean, C.M. (2020) Ball-and-chain inactivation in a calcium-gated potassium channel. *Nature*, *580*, 288–293.

Gasteiger, E., Hoogland, C., Gattiker, A., Duvaud, S., Wilkins, M.R., Appel, R.D., *et al.* (2005) Protein identification and analysis tools on the ExPASy server. In: Walker, J.M. (Ed.) *The proteomics protocols handbook*, Humana Press. pp. 571–607.

Golldack, A., Henke, B., Bergmann, B., Wiechert, M., Erler, H., Blancke Soares, A., *et al.* (2017) Substrate-analogous inhibitors exert antimalarial action by targeting the *Plasmodium* lactate transporter PfFNT at nanomolar scale. *PLoS Pathogens*, *13*, e1006172.

Haan, C. & Behrmann, I. (2007) A cost effective non-commercial ECL-solution for Western blot detections yielding strong signals and low background. *Journal of Immunological Methods*, *318*, 11–19.

Hapuarachchi, S.V., Cobbold, S.A., Shafik, S.H., Dennis, A.S., McConville, M.J., Martin, R.E., *et al.* (2017) The malaria parasite's lactate transporter PfFNT is the target of antiplasmodial compounds identified in whole cell phenotypic screens. *PLoS Pathogens*, *13*, e1006180.

Hormann, K. & Andreesen, J.R. (1989) Reductive cleavage of sarcosine and betaine by *Eubaterium acidaminophilum* via enzyme systems different from glycine reductase. *Archives of Microbiology*, *153*, 50–59.

Hoshi, T., Zagotta, W.N. & Aldrich, R.W. (1990) Biophysical and molecular mechanisms of Shaker potassium channel inactivation. *Science*, *250*, 533–538.

Hunger, D., Doberenz, C. & Sawers, R.G. (2014) Identification of key residues in the formate channel FocA that control import and export of formate. *Biological Chemistry*, *395*, 813–825.

Hunger, D., Röcker, M., Falke, D., Lilie, H. & Sawers, R.G. (2017) The C-terminal six amino acids of the FNT channel FocA are required for formate translocation but not homopentamer integrity. *Frontiers in Microbiology*, *8*, 1616.

Knappe, J. & Sawers, G. (1990) A radical route to acetyl-CoA: the anaerobically induced pyruvate formate-lyase system of *Escherichia coli*. *FEMS Microbiology Reviews*, *75*, 383–398.

Laemmli, U. (1970) Cleavage of structural proteins during the assembly of the head of bacteriophage T4. *Nature*, *227*, 680–685.

Lamiable, A., Thévenet, P., Rey, J., Vavrusa, M., Derreumaux, P. & Tufféry, P. (2016) PEP-FOLD3: faster de novo structure prediction for linear peptides in solution and in complex. *Nucleic Acids Research*, *44*, 449–454.

Leinfelder, W., Zehelein, E., Mandrand-Berthelot, M.A. & Böck, A. (1988) Gene for a novel tRNA species that accepts L-serine and cotranslationally inserts selenocysteine. *Nature*, *331*, 723–725.

Lowry, O., Rosebrough, N., Farr, A. & Randall, R. (1951) Protein measurement with the Folin phenol reagent. *Journal of Biological Chemistry*, *193*, 265–275.

Lü, W., Du, J., Schwarzer, N.J., Gerbig-Smentek, E., Einsle, O. & Andrade, S.L. (2012a) The formate channel FocA exports the products of mixed-acid fermentation. *Proceedings of the National Academy of Sciences USA*, *109*, 13254–13259.

Lü, W., Du, J., Schwarzer, N.J., Wacker, T., Andrade, S.L. & Einsle, O. (2013) The formate/nitrite transporter family of anion channnels. *Biological Chemistry*, *394*, 715–727.

Lü, W., Du, J., Wacker, T., Gerbig-Smentek, E., Andrade, S.L. & Einsle, O. (2011) pH-dependent gating in a FocA formate channel. *Science*, *332*, 352–354.

Lü, W., Schwarzer, N.J., Du, J., Gerbig-Smentek, E., Andrade, S.L. & Einsle, O. (2012b) Structural and functional characterization of the nitrite channel NirC from *Salmonella* Typhimurium. *Proceedings of the National Academy of Sciences USA*, *109*, 18395–18400.

Lv, X., Liu, H., Ke, M. & Gong, H. (2013) Exploring the pH-dependent substrate transport mechanism of FocA using molecular dynamics simulation. *Biophysical Journal*, *105*, 2714–2723.

Miller, J. (1972) *Experiments in molecular genetics*. Cold Spring Harbor, NY: Cold Spring Harbor Laboratory.

Mukherjee, M., Vajpal, M. & Sankararamakrishnan, R. (2017) Anion-selective formate/nitrite transporters: taxonomic distribution, phylogenetic analysis and subfamily-specific conservation pattern in prokaryotes. *BMC Genomics*, *18*, 560.

Peakman, T., Crouzet, J., Mayaux, J.F., Busby, S., Mohan, S., Harbourne, N., *et al.* (1990) Nucleotide sequence, organisation and structural analysis of the products of genes in the *nirB-cysG* region of the *Escherichia coli* chromosome. *European Journal of Biochemistry*, *191*, 315–323.

Peng, Y., Veneziano, S.E., Gillispie, G.D. & Broderick, J.B. (2010) Pyruvate formate-lyase, evidence for an open conformation favored in the presence of its activating enzyme. *Journal of Biological Chemistry*, *285*, 27224–27231.

Plaga, W., Frank, R. & Knappe, J. (1988) Catalytic-site mapping of pyruvate formate lyase: hypophosphite reaction on the acetyl-enzyme intermediate affords carbon-phosphorus bond synthesis (1-hydroxyethylphosphonate). *European Journal of Biochemistry*, *178*, 445–450.

Rossmann, R., Sawers, G. & Böck, A. (1991) Mechanism of regulation of the formate-hydrogenlyase pathway by oxygen, nitrate and pH: definition of the formate regulon. *Molecular Microbiology*, *5*, 2807–2814.

Saier, M.H. Jr., Eng, B.H., Fard, S., Garg, J., Haggerty, D.A., Hutchinson, W.J., *et al*. (1999) Phylogenetic characterization of novel transport protein families revealed by genome analyses. *Biochimica et Biophysica Acta (BBA) - Reviews on Biomembranes*, *1422*, 1–56.

Sambrook, J., Fritsch, E.F. & Maniatis, T. (1989) *Molecular cloning: a laboratory manual*, 2nd edition. Cold Spring Harbor, NY: Cold Spring Harbor Laboratory.

Sawers, G. & Böck, A. (1988) Anaerobic regulation of pyruvate formate-lyase from *Escherichia coli* K-12. *Journal of Bacteriology*, *170*, 5330–5336.

Sawers, G. & Böck, A. (1989) Novel transcriptional control of the pyruvate formate-lyase gene: upstream regulatory sequences and multiple promoters regulate anaerobic expression. *Journal of Bacteriology*, *171*, 2485–2498.

Sawers, G., Heßlinger, C., Muller, N. & Kaiser, M. (1998) The glycyl radical enzyme TdcE can replace pyruvate formate-lyase in glucose fermentation. *Journal of Bacteriology*, *180*, 3509–3516.

Schägger, H. & von Jagow, G. (1987) Tricine-sodium dodecyl sulfate-polyacrylamide gel electrophoresis for the separation of proteins in the range from 1 to 100 kDa. *Analytical Biochemistry*, *166*, 368–379.

Schägger, H. & von Jagow, G. (1991) Blue native electrophoresis for isolation of membrane protein complexes in enzymatically active form. *Analytical Biochemistry*, *199*, 223–231.

Soboh, B., Stripp, S.T., Muhr, E., Granich, C., Braussemann, M., Herzberg, M., *et al*. (2012) [NiFe]-hydrogenase maturation: isolation of a HypC–HypD complex carrying diatomic CO and CN- ligands. *FEBS Letters*, *586*, 3882–3887.

Suppmann, B. (1993) *Genetische Untersuchungen zum Formiat-Transport in Escherichia coli*. Dissertation, Ludwig-Maximilians-Universität Munich.

Suppmann, B. & Sawers, G. (1994) Isolation and characterisation of hypophosphite-resistant mutants of *Escherichia coli*: identification of the FocA protein, encoded by the *pfl* operon, as a putative formate transporter. *Molecular Microbiology*, *11*, 965–982.

Towbin, H., Staehelin, T. & Gordon, J. (1979) Electrophoretic transfer of proteins from polyacrylamide gels to nitrocellulose sheets: procedure and some applications. *Proceedings of the National Academy of Sciences USA*, *76*, 4350–4354.

Wagner, A.F., Frey, M., Neugebauer, F.A., Schäfer, W. & Knappe, J. (1992). The free radical in pyruvate formate-lyase is located on glycine-734. *Proceedings of the National Academy of Sciences USA*, *89*(3), 996–1000.

Waight, A.B., Czyzewski, B.K. & Wang, D.N. (2013) Ion selectivity and gating mechanisms of FNT channels. *Current Opinion in Structural Biology*, *23*, 499–506.

Waight, A.B., Love, J. & Wang, D.N. (2010) Structure and mechanism of a pentameric formate channel. *Nature Structural and Molecular Biology*, *17*, 31–37.

Wang, Y., Huang, Y., Wang, J., Cheng, C., Huang, W., Lu, P., *et al*. (2009) Structure of the formate transporter FocA reveals a pentameric aquaporin-like channel. *Nature*, *462*, 467–472.

White, W.B. & Ferry, J.G. (1992) Identification of formate dehydrogenase-specific messenger-RNA species and nucleotide-sequence of the *fdhC* gene of *Methanobacterium formicicum*. *Journal of Bacteriology*, *174*, 4997–5004.

Wiechert, M. & Beitz, E. (2017) Mechanism of formate-nitrite transporters by dielectric shift of substrate acidity. *EMBO Journal*, *36*, 949–958.

Zagotta, W.N., Hoshi, T. & Aldrich, R.W. (1990) Restoration of inactivation in mutants of Shaker potassium channels by a peptide derived from ShB. *Science*, *250*, 568–571.

SUPPORTING INFORMATION

Additional supporting information may be found online in the Supporting Information section.

How to cite this article: Kammel M, Hunger D, Sawers RG. The soluble cytoplasmic N-terminal domain of the FocA channel gates bidirectional formate translocation. *Mol Microbiol*. 2021;115:758–773. https://doi.org/10.1111/mmi.14641